USING WAVELETS ON DENOISING INFRARED MEDICAL IMAGES

Marcel S. Moraes, Tiago B. Borchartt, Aura Conci,
Computer Science Dep., Computer Institute, Federal
Fluminense University , UFF
Niteroi, Brazil
{msheeny, tbonini, aconci}@ic.uff.br

Trueman MacHenry
Department of Mathematics and Statistics,
York University
Toronto, Canada
machenry@mathstat.yorku.ca

***Abstract*—**This work presents the conclusions of an experimental study that intends to find the best procedure for reducing the noise of medium resolution infrared images. The goal is to find a good scheme for an image database suitable for use in developing a system to aid breast disease diagnostics. In particular, to use infrared images in the screening and postoperative follow-up in the UFF university hospital, and to combine this with other types of image based diagnoses. Seven wavelet types (Biorthogonal, Coiflets, Daubechies, Haar, Meyer, Reverse Biorthogonal and Symmlets) with various vanishing moments (such as Symmlets, where this number goes from 2 to 28, Daubechies from 1 to 45 and Coiflets 1 to 5) comprising a total of 108 different variations of wavelet functions are compared in a denoising scheme to explore their difference with respect to image quality. Three groups of Additive White Gaussian Noise levels (σ = 5, 25 and 50) are used to evaluate the relations among the approaches to threshold the wavelet coefficient (hard or soft), and the image quality after transformation-denoising-storage-decompression. Levels of decomposition are investigated in a new thresholding scheme, where the decision about the coefficient to be eliminated considers all variation, aiming for the best quality of reconstruction. Eight images of the same type and resolution are used in order to find the mean, median, range and standard deviation of the 432 combinations for each level of noise. Moreover, three evaluators (Normalized Cross-Correlation, Signal to Noise Ratio and Root Mean Squared Error) are considered for recommendation of the best possible combination of parameters.

***Keywords*—** *Gaussian noise, Infrared imaging, wavelet denoising, additive white Gaussian noise, adaptive noise reduction.*

I. INTRODUCTION

Medical procedures have become a critical area of application, which makes substantial use of image processing and, usually employs a great amount of data, need efficient content-based retrieval from image database, and improvements of image quality. Noise is a critical problem in biomedical images. However, it is not more important than its efficient storage and retrieval in clinics, hospitals or even repositories for research and development of computer aided diagnostic systems. Discrete wavelet based analysis combines facilities for these three features (denoising, storage and retrieval). This explains the importance of denoising procedure, based on a thresholding function. Such a technique has been integrated into DICOM standard for applications in compression and transmission of medical images. Moreover, at the same time that wavelets are a very powerful tool for multi-resolution analysis, they also allow introduce a broad combination of factors that should be analyzed to check their adequacy for the type of noise and image being focused on. Image restoration after storage and transition is fundamental for the quality of the other stages in the image processing (like segmentation, classification of the findings and recognition of elements) for diagnostic reports. Studies showed that infrared (IR) based image analysis could identify breast modifications earlier than other methods of examination [1, 16]. However, in order to be efficiently used, this type of imaging must first thoroughly analyze. Such analysis must consider a great number of patients, over a number of years; maintain record and make comparisons with others types of diagnoses, and combine and integrate data to allow mining possible conclusions for a computed aided prognostic (CAP) system [13-16].

Discrete wavelet transforms (DWT) have proven to be very effective in analyzing a very wide class of signals and images [6-9]. Wavelets allow a more accurate local description and separation of signal characteristics. DWT is a form that to reduces the storage area (because the coefficient and not the complete image, can be saved), at same time be used to improve the image quality, and promote content based retrieval of the data saved. Therefore, wavelet noise reduction techniques deserve to be investigated in such contexts. The main goal of the numerical experiments reported in this work is to identify the best wavelet approach to be used in a project of an image database on development to verify the possibilities of using infrared images in screening of breast diseases in a country with tropical climate. We have addressed this problem before for other types of medical imaging [5] or for using a reduced number of mother wavelets [12]. In this paper we improve the idea and the experimental study of using different wavelet implementations for a final conclusion about the best denoising methodology for digital infrared images. This result is currently being implemented in the project on the mastologic data base under development [13] for research on early breast cancer detection [16]. The obtained results are presented in graphs and tables, and used in a scheme to improve infrared image reconstruction.

The next section of this work describes aspects related to restoration in wavelet domain. Section 3 presents the data set used in our experimentations. Section 4 and 5 are related to

the results achieved with the DWT denoising techniques proposed for IR images. However they are separated in two types of texts. In section 4 we consider it in a group of images with a known level of noise results (to verify what is the best combination of factors on this specific application) while in section 5 real images where such a level of degradation is known is tested. Finally, section 6 reports the conclusions of this work.

II. On the Wavelet Denoising

Discrete wavelet transforms (DWT) have attracted more and more interest in biomedical image noisy reduction (denoising), storage and retrieval [2]. Denoising of images using wavelet is very effective because of its ability to capture the energy of a signal in few coefficients at various resolutions [7-10]. For traditional images, the wavelet transform yields a large number of small coefficients and a small number of large coefficients. In denoising, orthogonal sets with a single-mother wavelet function have played an important role. Due to merits of the localization of time-frequency characteristics and flexibility of choosing diverse methodologies; wavelet based restoration approaches have been considered for many applications of medical images and firmly established as a powerful denoising tool [2-5]. When used on images, DTW can be interpreted as 2D signal decomposition in a set of independent, spatially oriented frequency channels. The image in a spatial domain passes through two complementary filters and emerges in the frequency domain as coefficients of average and of details. The decomposed components could be assembled back into the original image domain without loss of information (Inverse Discrete Wavelet Transform - IDWT). The decomposed components could be processed before the image reconstruction, in order to improve the image or be used as a key for retrieving it in the image [6-8]. Generic denoising procedures using DWT involve three steps: *(i)* wavelet decomposition, *(ii)* threshold of coefficients related to noise in the wavelet domain and *(iii)* reconstruction by inverse wavelet transform into the spatial domain [9,10]. In the wavelet decomposition step, an image is decomposed into a sequence of spatial resolution images using DWT. In these, a given **j** level of decomposition can be performed resulting in **3j+1** different frequency bands of low (**L**) and high (**H**) components of the original image, namely, $\mathbf{LL^j}$, $\mathbf{LH^j}$, $\mathbf{HL^j}$ and $\mathbf{HH^j}$, as shown in Fig. 1 [7].

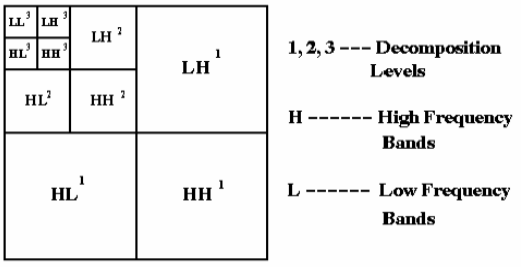

Fig. 1. DWT decomposition in three (j=3) levels of high and low sub bands.

Variations of DWT are based on diverse selection of this level of decomposition. According to image characteristics a good level could be defined in order to reduce the computation time and the production of redundant elements. The goal of this decomposition is to start from a resolution oriented decomposition, and then to analyze the obtained signals on frequency sub-bands. It corresponds to a tree decomposition scheme, in which the result of each filtering process serves as input to the next. This generates a tree structure from an initial image, which is decomposed (in the first level j = 1) into coefficients of averaged information (cA1, from a low pass filter) and coefficients of details (cD1, from a high pass filtering). The detail coefficients could be in vertical, horizontal and diagonal directions: cD1(v), cD1(h) and cD1(d). These turn again into approximations and details of next level (j = 2), and so on (j = 3, 4,…), until a given number of levels of decompositions is reached [7]. The discrete wavelet transform is characterized by the used type of wavelet function ("wavelet-mother"), as well. Figure 2 shows some wavelet mother used in this work.

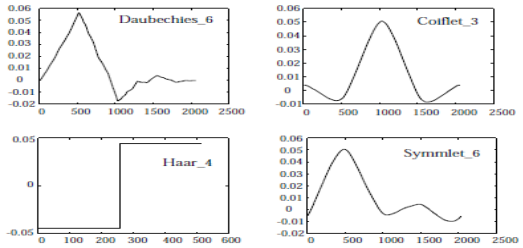

Fig. 2. Some used wavelet.

Each one of these offers a particular way of coding signals or images in terms of preserved energy, and reconstructed features. A family of functions is used recursively with pairs of conjugate filters (low and high pass filters). Among all admissible bases, a particular one is selected by choosing how they are decomposed by means of the conjugate filters. At each level four decompositions are possible, so the results have a quadtree structure as it is shown in Fig. 3.

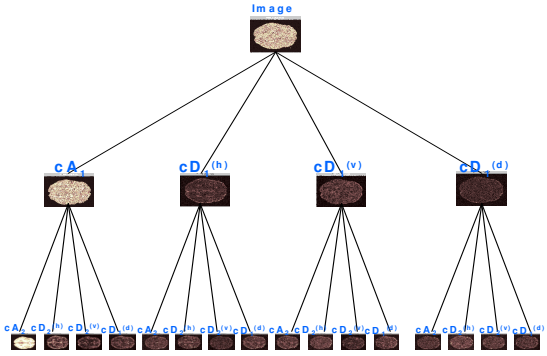

Fig. 3. Decomposition of DWT of two levels

Then, by combining level and wavelets types, DWT can be used in a lot of ways for a given image. These offer a flexible tool for analysis, when the coefficients of details (cD related with **H**) as well as the average coefficients (cA related to **L**) are separated in a fine or at a coarser scale (depending on **j**). Moreover, there are yet more possibilities for analysis in DWT

scale-oriented decomposition of the frequency sub bands. Among them is the possibility of defining rules related to how some coefficient, that is less than a particular value (threshold), is set to zero. This is based on where the most relevant aspect for denoising (low or high frequency elements) of a given type of image is, and how the process of defining them at zero can be established [6].

Adequate image compression consists of setting to zero values of the coefficients which are considered negligible. It could be done by two different kinds of methods, considering a suitable threshold chosen in advance. The difference between then is that in one the detail coefficients whose magnitude is larger than the threshold are kept without modification (hard-threshold methods), while in the other they are shrunk towards zero (soft-threshold methods). These are named *Hard* thresholding and *Soft* thresholding techniques [7,9]. The Hard thresholding is given by the scheme in Fig. 4, where δ is the threshold value. Soft thresholding consists of deleting some coefficients and at same time reducing the others in order to promote a gradual transition. Soft thresholding wavelet coefficients are done by the scheme in Fig. 5, where δ is the threshold value, and *sgn( )* is the *signal function* (its value 1 when the argument is up to zero and -1 otherwise). In both cases, the threshold value δ is critical in determining which coefficients will be retained or discarded.

$$y_{hard}(t)=\begin{cases} x(t), & |x(t)|>\delta \\ 0, & |x(t)|<\delta \end{cases}$$

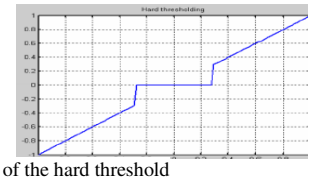

Fig. 4. Scheme of the hard threshold

$$y_{soft}(t)=\begin{cases} \mathrm{sgn}(x(t))\cdot(|x(t)-\delta|), & |x(t)|>\delta \\ 0, & |x(t)|<\delta \end{cases}$$

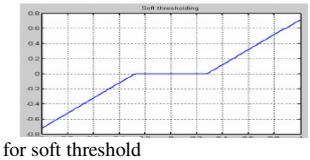

Fig. 5. Scheme for soft threshold

Denoising images corrupted by an Additive White Gaussian Noise (AWGN) using DWT follows the same idea of threshold for image compression. Since the works of Donoho [7] and Donoho and Johnstone [8,9] on threshold coefficients for restoration many methods have been proposed and used resulting in a great number of DWT denoising approaches. As has being mentioned before, after the coefficients have been suppressed, inverse wavelet transformation is carried out to reconstruct the image. Hard thresholding is simpler, but for many types of images soft thresholding offers better denoising results.

III. TECHNIQUES USED

In this work, hard and soft thresholding are tested. Moreover, we present a new method for choosing the coefficients to be modified (specifically tailored for the quality of the reconstructed image), and compared it with all possible combination of the other options. They are represented in the tables, graphs and figures in Section 3, and identified by adequate abbreviations that intend to represent the used characteristics. All of the possible combinations of characteristics have been tested separately for eight different images acquired in conditions very similar to those in use for the breast exams and processes on similar conditions in the same computer environment as the wavelet process.

The main intention of this work is to find the best combination among the level of decomposition, type of wavelet function and threshold to achieve the best result on denoising infrared images depending on its noise level. To achieve this, a series of experiments using the steps presented in Fig. 6 is made. In these, three known level of noise has been synthetically added to the set of images to be analyzed. Resulting in 32 images of same type separated into 4 groups with respect to the levels of noise (0, 5, 25 and 50).

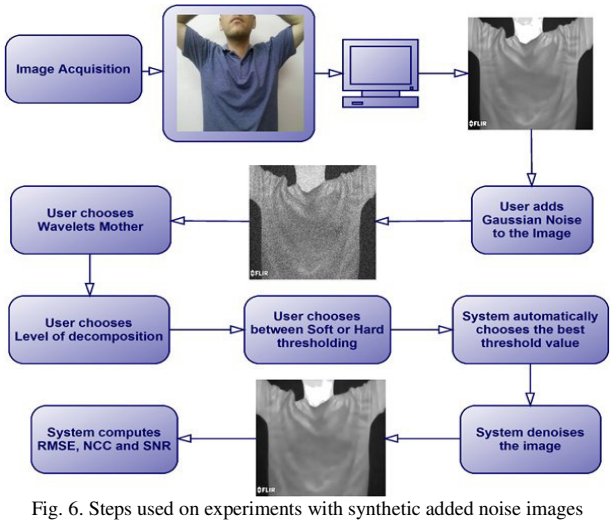

Fig. 6. Steps used on experiments with synthetic added noise images

The thresholding method proposed is not based *on a unique value* δ for threshold, but by testing all possibilities for achieving better quality of the denoised image. Values of the threshold in a series of possibilities δ(**n**) are defined and related to each element **n** of this series. To consider the reconstructed image quality the normalized cross correlation (NCC) between the original and the denoised images is estimated. In this case when the images are more correlated the better is the δ.

Then, with all others parameters defined, the best threshold value for a given image is found automatically by the system considering best quality possible for the restored image. Such a search is put into an admissible computational length of time by using discrete possibilities previously delimited (*e.g.* it is set to 256 elements for most of the experimentations done). That is, the discrete δ(**n**) is organized in an array where the best δ is found by a function of complexity O(log(**n**)).

This novel approach to estimate the threshold adaptively is implemented using the Matlab environment and verifying all coefficients up to a previously defined level, **j**. Figure 7 shows the relation among NCC and the thresholding index for

the case of Biorthogonal 1.3, level 4 and hard threshold. The threshold value δ is obtained by associating (using the Matlab functions [11] it with a series of discrete possibilities δ(**n**), as it is described in the following. The main idea of this process is: First, use in the noise image random threshold level (**n**) and define for δ a discrete number of possibilities: δ(**n**). Using a specific value **n** the restoration process is done considering δ(**n**) and the reconstructed image quality by computing its NCC (related to the original image). The same process is executed for all threshold index (0, ..., **255**) and the best threshold is archived by looking the best NCC value. As this process could take some time, an optimization procedure based on the merge sort algorithm was implemented. This produces results in an algorithm with computational complexity of order log(**n**), *i.e* O(log(**n**)).

Figure 6 presents the steps used in the experiments performed using Matlab R2011b (Mathworks Inc.). See Wavelets Toolbox for definition of the best combination of the parameters considering the noise level [11]. These are:

Step 1: Image acquisition and storage as raw data. When evaluated by the common techniques used when dealing with noise as a criterion, all original images are considered without noise.

Step 2: Gaussian noise addition to the original images of Step 1. Three levels of a standard deviation value (σ_{noise} = 5, 25 and 50) are added.

Step 3: This step is divided into four (4) sub-steps, in the first three the user defines the type of wavelet to be employed on the decomposition (Coifflets, Bi-orthogonal, Symmlets, etc.), the level of adaptive decomposition from **j** up to level **j**+1 and the threshold process to be applied to modify properly the wavelets coefficients. Then the used system selects automatically the coefficient threshold based on the NCC that produces greater correlation between the original and the reconstructed image.

Step 4: Image restoration: Using the modified coefficients the image in the spatial domain is reconstructed by applying the inverse wavelet packet transform.

Step 5: Verification or validation of the process (resulting from Step 4) is done by comparing the reconstruction with the free-of-noise original image.

Three validation criteria are used: Normalized Cross Correlation (NCC), Signal to Noise Ratio (SNR), and Root Mean Square Error (RMSE) for comparison between the original and the denoised image.

Let us stress further the novel aspects of this sketched: This use of a variable threshold for each image in order to maintain its quality; also the number of coefficients to keep is not fixed. This simple idea as far as we know have not bee used before, because its implementation is a little bit more complex. Differently of all others works, we do not use a fixed value δ for the threshold and we test all possibilities for achieving a better denoised image. Values of threshold in a series of possibilities δ(n) are defined and related to each element n of this series. To consider the reconstructed image quality the normalized cross correlation (NCC) between the original and the denoised images is estimated. This values result in a curve like figure 7 for each image, where 256 possibilities was tested experimentally. These figures present an optimal point where the NCC value goes to a maximum. For instance, in figure 7, it corresponds to a combination of δ(80). Then the best threshold value for a given image is found considering the quality based in the NCC of the restored image. Such search is put into an admissible computational time frame by using discrete possibilities, previously defined (256 elements for such experimentations). That is, the discrete δ(n) is organized in an array where the best threshold is found adaptively considering all wavelet coefficients up to a previously defined level, j of the wavelet. Section 3 presents the results of these experimentations.

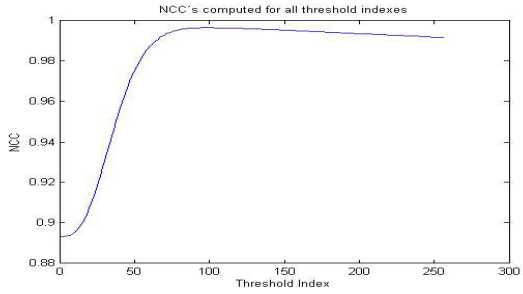

Fig 7. Example of the concave function relating threshold index and NCC for the best result of the base Biorthogonal 1.3.

IV. RESULTS CONSIDERING A KNOWN LEVEL OF NOISE GAUSSIAN NOISE (AWGN) FUNCTION.

Adequate estimation of noise level in real images is challenging due to the great variation among the available approaches to measure it [6]. In order to have a "ground truth" for experimentations, in all images used, the noise is synthetically add at different degradation level. Theses levels correspond to the standard deviation of the noise (σ = 5, 25 e 50) added to the original infrared images by using an Additive White Gaussian Noise (AWGN) function. All image used are acquired by a Flir SC620 camera (with sensibility of 0.08º Celsius) in 640x480 resolution and encoded using 8 bit per pixels. Figure 8(a) shows an example of one image when it can be considered free of noise. These images are also submitted to the usual noise evaluation approaches [2, 10] and no part of them presents measurable noise values.

TABLE I. USED WAVETETS

Bior 1.1	Bior 3.7	db 1	db 11	db 21	db 31	db 41	rbio 2.2	rbio 5.5	sym 10	sym 20
Bior 1.3	Bior 3.9	db 2	db 12	db 22	db 32	db 42	rbio 2.4	rbio 6.8	sym 11	sym 21
Bior 1.5	Bior 4.4	db 3	db 13	db 23	db 33	db 43	rbio 2.6	sym 2	sym 12	sym 22
Bior 2.2	Bior 5.5	db 4	db 14	db 24	db 34	db 44	rbio 2.8	sym 3	sym 13	sym 23
Bior 2.4	Bior 6.8	db 5	db 15	db 25	db 35	db 45	rbio 3.1	sym 4	sym 14	sym 24
Bior 2.6	coif 1	db 6	db 16	db 26	db 36	Dmey	rbio 3.3	sym 5	sym 15	sym 25
Bior 2.8	coif 2	db 7	db 17	db 27	db 37	Haar	rbio 3.5	sym 6	sym 16	sym 26
Bior 3.1	coif 3	db 8	db 18	db 28	db 38	rbio 1.1	rbio 3.7	sym 7	sym 17	sym 27
Bior 3.3	coif 4	db 9	db 19	db 29	db 39	rbio 1.3	rbio 3.9	sym 8	sym 18	sym 28
Bior 3.5	coif 5	db 10	db 20	db 30	db 40	rbio 1.5	rbio 4.4	sym 9	sym 19	-

Figures 8(b), (c) and (d) show the image of Fig. 8(a) after addition of tree noise levels: low, medium and high. In a similar way, a small database of 32 different images was created, each one with a known level of noise. Each noise added image is analyzed considering the steps for identification of the best wavelet denoising characteristics described in previous section (Fig. 7). A total of 108 different bases is used (it is important to remember here that, in fact, Haar and Daubechy 1 is the same base), as shown in Table I. In this work they are abbreviated as Bior = Biorthogonal, coif = Coiflets, db = Daubechies, Dmey = Discrete Meyer, rbio = Reverse Biorthogonal, and sym = Symmlets.

For the 8 images, each of the 108 bases are tested for levels 3 and 4 of the decomposition (L3 and L4), and the 2 possible way of coefficient thresholding (soft and hard). Each configuration has been considered for the images with added Gaussian noise at three different levels of standard deviation (5, 25 and 50), with the best thresholding value automatically computed, resulting in a total of 10,368 experiments. Figure 9 shows the worst and best result for each level of noise of these images. Based on such visual results, for all noise levels, the proposed method presents adequate denoising proprieties considering the best results. Quantitative study is required to verify the potential difference among each of the possibilities. For each configuration, three evaluators are considered: NCC, SNR and RMSE. Tables II and III summarize the results related to them. Comparing both visual and numerical evaluation, the denoised images obtained is adequate when SNR>20, RMSE<7 and NCC>0.99.

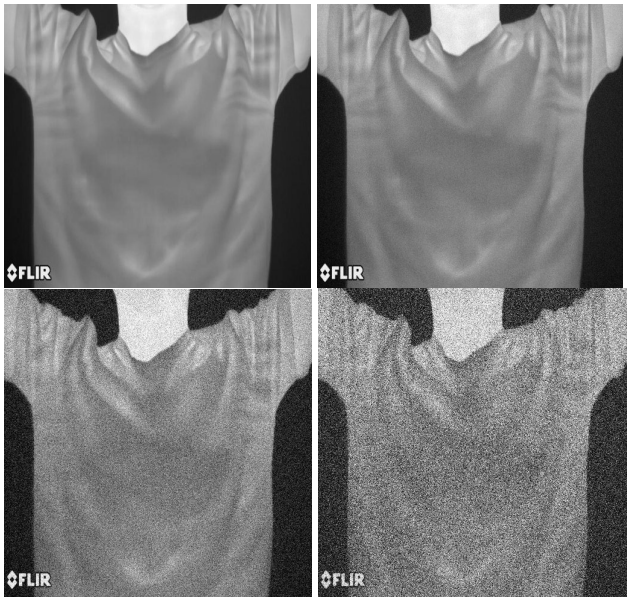

Fig. 8. Sample of original image and noisy image perturbed by noise level of noise (σ =5, 25 and 50) used in experiments

To facilitate a comparative analysis of these values, results from each measure were normalized and averaged for all images on the same noise level. These values are shown in the graph of Fig. 10. This figure allows for the consideration that all measures (SNR, RMSE and NCC) follow a pattern. Then in further analysis only the data from the NCC are considered here. However, complete data for all measures can be accessed at www.ic.uff.br/visuallab. Considering the position of each base on Tab. I as reference, Tab. IV describes the average values of NCC for each base on all noise levels. In table 4 each wavelet are represented by its position in Table I. Colors from **green** to **red** are used to grade these results visually. From this table, it can be inferred that the base with the worst result was the Reverse Biortogonal 3.1 (rbio3.1 in Table IV), while the best was Biortogonal 1.3 (Bior1.3 in Table V).

The top 10 configurations tested considering the 3 measures (NCC, SNR and RMSE) and the noise level can be compared in Table V for the low noise level that is for (Gaussian noise 5). Analyzing the 3 measures NCC, SNR and RMSE, in order of importance, the top 10 settings present results very similar. It is possible to see that of the 10 best results on removing noise level 5, are found using hard thresholding, which is in all cases better than soft thresholding. The use of Level 3 or Level 4 of decomposition makes practically no difference for low level of noise. However, when analyzing the influence of the level on the top 50 results, as done in Fig. 11, it is possible to see that for the same noise level the decomposition on Level 4 usually present better results then Level 3. This is the unique previous expected result on these experimentations.

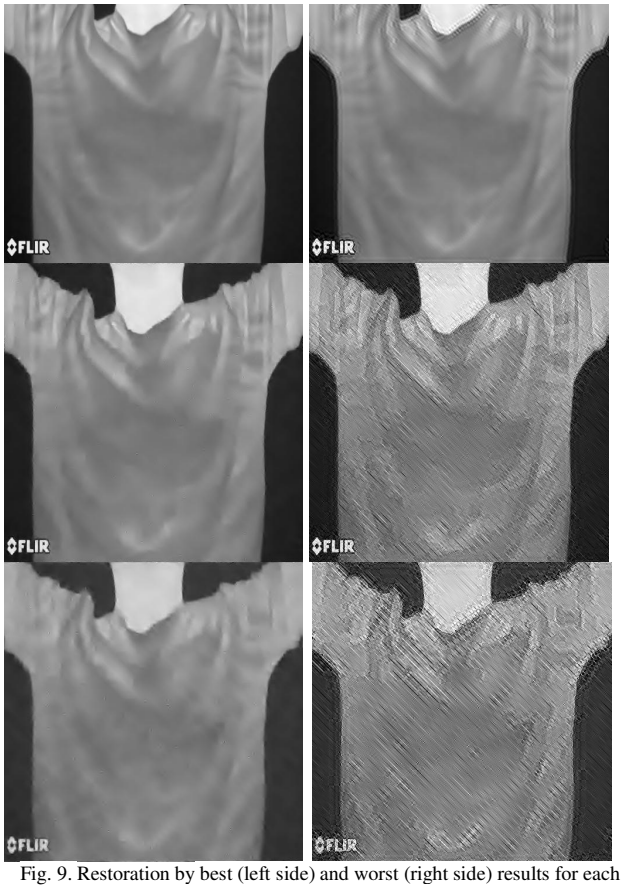

Fig. 9. Restoration by best (left side) and worst (right side) results for each level of noise using the scheme presented in section 2.

TABLE II. RESULTS FOR THE BEST CASE OF EACH NOISE LEVEL.

σ	W.type	l.	H\S	Tindex	SNR	RMSE	NCC
5	coif 1	3	h	18	117.865	1.098	0.999
25	bior 1.3	4	h	98	33.615	3.857	0.996
50	bior 1.3	4	h	183	16.850	7.611	0.989

TABLE III. RESULTS FOR THE WORST CASES OF EACH NOISE LEVEL.

σ	W.type	leve	H\S	T. index	SNR	RMSE	NCC
5	rbio 3.3	3	h	129	39.692	3.174	0.994
25	rbio 3.1	4	h	80	14.757	8.641	0.910
50	rbio 3.1	4	h	189	12.708	10.145	0.757

TABLE IV. COMPARISON OF THE AVERAGE NCC VALUES FOR ALL IMAGES ON ALL NOISE LEVEL FOR THE USED DENOISING METHODS.

	A	B	C	D	E	F	G	H	I	J	K
1	0.9933	0.9896	9933	0.9906	0.9897	0.9891	0.9887	0.9908	9927	0.9915	0.9911
2	0.9938	0.9897	9925	0.9905	0.9896	0.9891	0.9886	0.9905	9917	0.9914	0.9911
3	0.9937	0.9917	9922	0.9903	0.9895	0.9890	0.9886	0.9901	9925	0.9914	0.9910
4	0.9921	0.9894	9919	0.9902	0.9895	0.9890	0.9886	0.9898	9922	0.9913	0.9909
5	0.9924	0.9918	9916	0.9901	0.9894	0.9889	0.9885	0.9308	9922	0.9913	0.9910
6	0.9924	0.9925	9913	0.9901	0.9894	0.9889	0.9909	0.9863	9920	0.9912	0.9911
7	0.9923	0.9921	9912	0.9900	0.9893	0.9888	0.9933	0.9877	9919	0.9912	0.9910
8	0.9705	0.9919	9910	0.9899	0.9893	0.9888	0.9933	0.9874	9917	0.9912	0.9908
9	0.9868	0.9917	9908	0.9898	0.9892	0.9888	0.9920	0.9871	9917	0.9912	0.9935
10	0.9890	0.9915	9907	0.9897	0.9892	0.9887	0.9916	0.9925	9916	0.9910	-

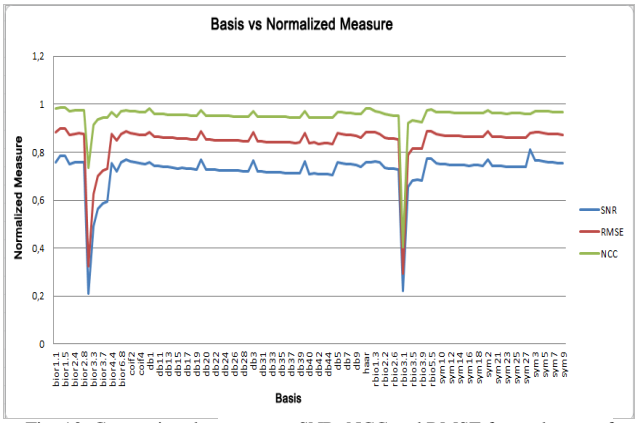

Fig. 10. Comparing the measures SNR, NCC and RMSE for each type of wavelet used.

The most important conclusion considering all the computation done is that the type of used wavelet presents no importance on low noise level but its importance increase according the level of noise. The seven most relevant are the Coiflet 1, Symmlet 2, Daubechie 2, Symmlet 3, Daubechie 3, Biortogonal 2.6 and Reverse biortogonal 5.5. The hard threshold is usually better, and that for low level of noise only the three levels of decomposition can be used.

When analyzing the influence of hard or soft threshold in the top 50 results (as done in Fig. 12) it is possible to state that for the same base in all levels of noise hard threshold usually has an advantage over soft threshold. This is very interesting because hard threshold is a simpler and faster approach. Although it is difficult to find works that like ours go further in depth discussion on same analysis on this comparison of hard and soft thresholds in the result. Same kind of results has appeared on other type of medical images for our group [15].

TABLE V. THE 10 BEST COMBINATIONS FOR LOW NOISE LEVEL.

Base	Level	H/S	NCC	SNR	RMSE
Coif 1	L3	H	0.999557	117.865253	1.133402
Coif 1	L4	H	0.999552	117.273865	1.146983
Sym 2	L3	H	0.999551	117.129401	1.135497
Db 2	L3	H	0.999551	117.129401	1.135497
Sym 3	L3	H	0.999548	116.427425	1.14867
Db 3	L3	H	0.999548	116.427425	1.14867
Sym 2	L4	H	0.999547	116.664894	1.148594
Db 2	L4	H	0.999547	116.664894	1.148594
Bior 2.6	L4	H	0.999547	116.628034	1.142708
Rbio 5.5	L4	H	0.999547	116.483195	1.143878

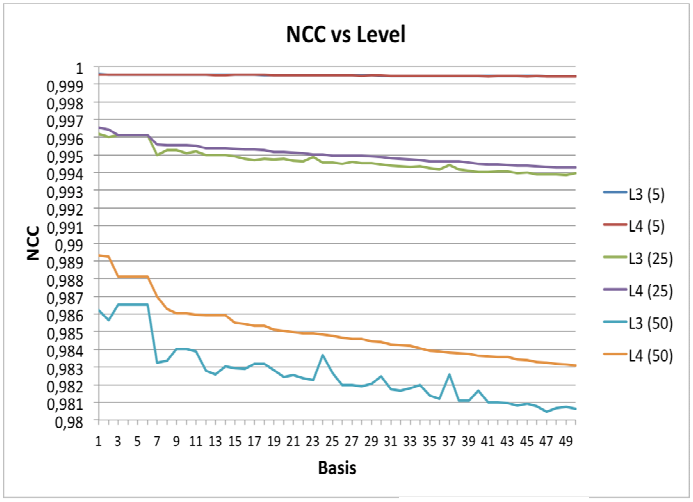

Fig. 11. NCC values considering noise and level of decomposition.

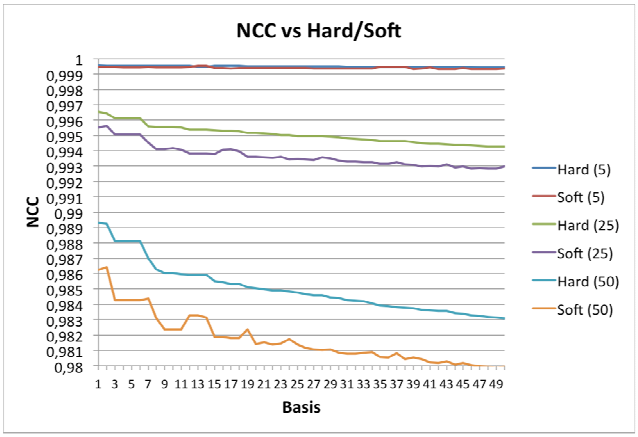

Fig. 12. NCC for each base, level of noise and type of thresholding.

V. RESTORATION OF INFRARED OF WHATEVER NOISE LEVEL

In this section, a brief description of how the last section results can be used in denoising infrared images with unknown

level of noise is provided. As the Coiflet 1 base presents the best characteristic for all noise level, only this is the implemented in our final project database for infrared images. The same occur with the hard threshold scheme that is the unique approach considered. The noise level is important on the consideration of using level 3 or 4. Then it must be first roughly evaluated to verify approximately if it presents standard deviation, σ, above 20. In such case the level of decomposition is set as 4 and, it is to 3 in other case. Usually, biomedical images are considered corrupted by white additive Gaussian noise which is characterized by the noise variance σ, that could be estimated from the theorem of Donoho and others methods by using one or more images [8]. A relatively simple approach to estimate the noise variance is to use the difference between two matched images of the same object [4]. Although the technique is simple to be implement, its efficiency relies heavily on the correct alignment of the two images. Therefore, most of the times in image processing techniques that use a single image are preferred. Some methods using a single image are based on manual selection of uniform signal or non signal regions [5]. However such techniques are time consuming and have a high intra and inter user variability. Previous section shows that the level of decomposition is only relevant for medium of higher level of noise and as in dynamic acquisition protocol a series of images of the same patient in obtained at almost same position [1], the subtraction method is used to verified if the image on analysis present more noise then one of the same type with σ=20 (by using simple technique of standard deviation computation [5]). If the answer is positive, the system set for level 4 of decomposition on the other case level 3 is used. Figure 13 presents the steps suggested on performing an efficient restoration scheme for infrared images considering the noise level. They are:

Step 1: Image acquisition and storage as a raw data;
Step 2: Evaluation of noise level and decision about decomposition in level 3 or 4;
Step 3: Coiflet wavelet and hard threshold are used;
Step 4: Coefficients for thresholding is select automatically based on the NCC;
Step 5: The image is reconstructed using the modified coefficients.

Figure 14 shows, from left to right, typical IR acquired [1,16,18], original to be used in the database and its denoised version. Table VI compares the second and third image on Fig. 14 with the first in terms of quality and size of the file to the used in the database. Time of processing this is **0.4063** seconds. The image needs now 68.79% less space for storage. Its quality improves more then 2.7 times considering the SNR, RMSE and 1.2 times considering the NCC evaluator. For this storage a simple **jpeg** format is used, that is not only the DWT coefficient are saved (this could reduce greatly more the file size but is opposite to the idea of a completely public database, using a common **jpeg** format every body can use the images for researches).

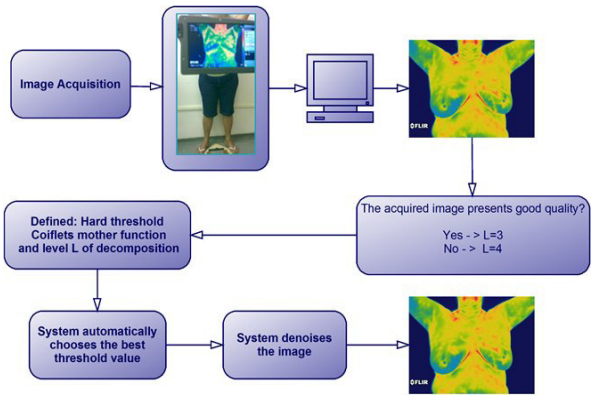

Fig. 13. Proposed restoration steps for IR images.

Fig. 14. Original acquired image with size: 49,519 bytes (left), image after storage and transmission: 50,846 byte (center) and denoised image by the proposed scheme: 15,869 bytes (right).

TABLE VI. COMPARING ACHIEVED RESULTS FOR TYPICAL BREAST IMAGE.

Fig 14	SNR	RMSE	NCC	Size (bytes)
Left-center	5.9197	2.2273	0.8202	50,846
left- right	16.0751	0.8202	0.9997	15,869

VI. CONCLUSIONS

Methods using wavelets has become very important in biomedical image researches for improve image based diagnosis in many ways from the initial storage and transmission possibilities, passing by the retrieval of the information based on the image content and going up to the possible image quality improvement by promoting its noise reduction. On such aspects, the JPEG2000 part II standard that is designed to support medical image compression and transmission applications is based on the discrete wavelet transform using the Daubechies (9,7) biorthogonal wavelet (also known as Cohen- Daubechies-Feauveau 9/7). However, this could not be the best possible wavelet for every conditions and kind of images.

This work tries to find the best combination of wavelet based denoising parameters for medium resolution (640 x 480) infrared image acquired by a FlirSC620 camera (considering a human being distant from 1 to 1.2 meters). In order to verify this, results of experiments from 108 different bases and 1296 denoising schemes are performed to compare their difference. They are analyzed considering low, medium and high levels of Additive White Gaussian Noise. The performance of each approach is evaluated by comparing the originals without noise versus the same images after compression/denoising and decompression using all possible combination of aspect. Three well known measures are used to evaluate the relation among fidelity they are: Root mean square error, signal to noise ratio and the normalized cross correlation. The decomposition is

tested on two levels (3 and 4) of the image wavelet coefficients representation. They are reconstructed after compression and denoising by hard and soft coefficient modifications by thresholding. The goal is to grade combinations of processes considering the visual quality. Although, in all tested images hard threshold present best results considering the visual quality for all parameters. Decomposition up level 3 presents same results than decomposition up level 4 for low level of noise. All testes realized consider Coifelet 1 the best wavelets. Slightly worse results are achieved by Symmlet 2, Daubechie 2, Symmlet 3, Daubechie 3, Biortogonal 2.6 and Reverse biortogonal 5.5. It is observed that higher the noise level the greater is the difference among all methodologies. In averaging the images for each others aspect of the methods, the measures presents equally well when they are grading of the best to the worst results. That is SNR, RMSE and NCC values, follows the same orders for each method. However, according to the results shown in Tables IV and V and in Figures 11 and 12, as the images become harder to be restored (higher noise level), the difference among all methodologies gets larger. The difference on computational demands and time among approaches is no relevant (they are very imperceptible). For the hardest images in this restoration sense (i.e. $\sigma = 25$ and 50), the order of the 10 best results reveal the same of those with smaller noise level and more simple degradation. This behavior leads us to think that is possible to advise best form for image denoising for all level of noise contained using the automatic selection of parameters based on the a more efficient results and relating the noise level only to the control of the level of decomposition (such scheme becomes an approach presented and tested in the second series of results). That is based on the experimentations an efficient and fast denoising approach is proposed and tested for breast infrared images with unknown level of noise. In order to turn possible to choose the threshold values based on the image reconstructed quality an new method for threshold definition based on series of $\boldsymbol{n}$ discrete possibilities is presented. The quality is considered represented by the NCC (or any other measure) between original and denoised image. The main advantage of this method is its low level of computational complexity, which is of order $O(log(\boldsymbol{n}))$ and its robustness. Although the experimentation and denoising approach proposed are performed for IR images, the presented idea is generic for wavelet based restoration and can be used of other type of images to found algorithms most appropriated, related to the noise level, type of decomposition and threshold to be used.

ACKNOWLEDGMENT

This research has been partially supported by the Brazilian agencies FAPERJ, CAPES and CNPq. It is part of the MACC and the SiADDi-E projects.

REFERENCES

[1] T. B. Borchartt, A. Conci, R.C.F. Lima, R. Resmini, A. Sanchez, "Breast thermography from an image processing viewpoint: A survey", Signal Processing , Vol. 93, No. 10, pp. 2785-2803, 2013.

[2] S. Aja-Fernandez, C. Alberola-Lopez, C. F. Westin, "Noise and signal estimation in magnitude MRI and Rician distributed images: A LMMSE approach", IEEE Transactions on image processing, Vol. 17, No. 8, pp. 1383-1398, 2008.

[3] S. Basu, T. Fletcher and R. Whitaker, "Rician noise removal in diffusion tensor MRI", in Proc. MICCAI, Vol. 1, pp. 117–125, 2006.

[4] P. Coupé, J.V. Manjón, E. Gedamu, D. Arnold, M. Robles and D. Louis Collins, "Robust Rician noise estimation for MR images", Medical Image Analysis, Vol. 14, No. 4, pp. 483-493, 2010.

[5] G. Pérez, A. Conci, A. B. Moreno, J. A. Hernandez-Tamames, "Rician Noise Attenuation in the Wavelet Packet Transformed Domain for Brain MRI", Integrated Computer-Aided Engineering, Vol 21, Number 2, 163-175, 2014.

[6] L. Birgé and P. Massart. "From model selection to adaptive estimation", In: D. Pollard, E. Torgersen and G.L. Yang (eds), Festschrift for Lucien Le Cam, Springer-Verlag, 1997.

[7] D.L. Donoho, "De-Noising by Soft-Thresholding", IEEE Trans. Inform. Theory, pp. 613-627, 1995.

[8] D.L. Donoho and I.M. Johnstone, "Adapting to unknown smoothness via wavelet shrinkage", Journal of American Statistical Assoc., Vol. 90, No. 432, pp. 1200-1224, 1995.

[9] D.L. Donoho and I.M. Johnstone, "Ideal spatial adaptation via wavelet shrinkage", Biometrika, Vol. 81, No. 3, pp. 425-455, 1994.

[10] C.S. Anand and J.S. Sahambi. "Wavelet domain non-linear filtering for MRI denoising", Magnetic Resonance Imaging, Vol. 28, pp. 842–861, 2010.

[11] MathWorks, "Documentation Center: wbmpen", 2012. Available at:

[12] <http://www.mathworks.com/help/wavelet/ref/wbmpen.html>.

[13] Moraes, M.; Borchartt, T.B. ; Conci, A.; Kubrusly, C. , "On Efficient Use of Wavelet In Infrared Image Database", IWSSIP 2013, IEEE Xplore Conference Proceedings, 31-34, 2013.

[14] http://ieeexplore.ieee.org/xpl/articleDetails.jsp?arnumber=6623442.

[15] L. F. Silva, D. C. M. Saade, G. O. Sequeiros, A. C. Silva, A. C. Paiva, R. S. Bravo and A. Conci, "A new database for mastology research with infrared image", Journal of Medical Imaging and Health Informatics, Vol 4, No. 1, pp.92-100, 2014.

[16] Rodrigues, E.O.; Conci, A.; Borchartt, T.B.; Paiva, A.C ; Correa Silva, A. ; MacHenry, T. "Comparing results of thermo graphic images based diagnosis for breast diseases", IEEE International Conference on Systems, Signals and Image Processing, pp. 39-42 IEEE Xplore http://ieeexplore.ieee.org/xpl/mostRecentIssue.jsp?punumber=6824677, 2014

[17] R. Souza Marques, A. Conci, T. Machenry, "On the use of Hausdorff Distance on Evaluation of Breast Image segmentations", Biomat 2013. – Field Institut, Toronto. http://www.biomat.org/biomat2013/indexbiomat2013.html

[18] L.A. Bezerra, M. M. Oliveira, M. C. Araújo, M. J. A. Viana, L. C. Santos, F. G. S. Santos, T. L. Rolim, P. R. M. Lyra, R. C. F. Lima, T. B. Borschartt, R. Resmini, and A. Conci, "Infrared Imaging for Breast Cancer Detection with Proper Selection of Properties: From Acquisition Protocol to Numerical Simulation", pp. 285-332. Chapter: 11. In: Multimodality Breast Imaging: Diagnosis and Treatment Editors: E. Y. K. Ng; U. R. Acharya; R. M. Rangayyan; J. S. Suri. Bellingham, Washington, USA, SPIE, 2013.